Journal of Organometallic Chemistry, 402 (1991) 113–123
Elsevier Sequoia S.A., Lausanne
JOM 21231

Penta- and heptanuclear π-toluene derivatives of ruthenium

Karen J. Edwards, John S. Field, Raymond J. Haines * and Faizel Mulla
Unit of Metal Cluster Chemistry, Department of Chemistry, University of Natal, P.O. Box 375, Pietermaritzburg (Republic of South Africa)

(Received June 19th, 1990)

Abstract

Reaction of $[Ru_3(CO)_{12}]$ with $PPhH_2$ in toluene under reflux affords a range of higher nuclearity as well as trinuclear products, two of which have been characterised as the π-toluene derivatives $[Ru_5(\mu_4\text{-}PPh)(CO)_{12}(\eta^6\text{-}C_6H_5Me)]$ and $[Ru_7(\mu_4\text{-}PPh)_2(CO)_{15}(\eta^6\text{-}C_6H_5Me)]$. Crystal structure determinations have revealed that the structures of these two compounds are based on those of their parents, $[Ru_5(\mu_4\text{-}PPh)(CO)_{15}]$ and $[Ru_7(\mu_4\text{-}PPh)_2(CO)_{18}]$, with three carbonyls on one of the ruthenium atoms of each cluster having been replaced by a π-toluene ring.

Introduction

An established method of synthesis of arene metal carbonyl derivatives involves the direct reaction of arenes with metal carbonyls under appropriate reaction conditions. Thus treatment of the hexacarbonyls of chromium, molybdenum or tungsten with arenes such as benzene, toluene, xylene, mesitylene and naphthalene at elevated temperatures leads to the formation of products of the type $[M(CO)_3(\eta^6\text{-arene})]$ (M = Cr, Mo or W) in good yield [1,2]. This procedure is not restricted to mononuclear derivatives and thus the reaction of $[Ru_3(CO)_{12}]$ with mesitylene in n-hexane or n-heptane under reflux has been shown to afford the hexanuclear species $[Ru_6(\mu_4\text{-}\eta^2\text{-}CO)_2(CO)_{13}(\eta^6\text{-}C_6H_3Me_3)]$ in low yield [3]. Reactions of this type also lead to the formation of products containing interstitial carbide ligands with the yield of these species being dependent on the reaction temperature [3,4]. Thus while $[Ru_6(\mu_4\text{-}\eta^2\text{-}CO)_2(CO)_{13}(\eta^6\text{-}C_6H_3Me_3)]$ is the sole product of the above reaction in hexane under reflux, the carbido-cluster $[Ru_6(C)(CO)_{14}(\eta^6\text{-}C_6H_3Me_3)]$ is the only product of the corresponding reaction in refluxing n-nonane or n-octane [3]. In general, arenes bond to a single metal atom in metal clusters, via a conventional η^6 co-ordination mode as found in $[Ru_6(C)(CO)_{14}(\eta^6\text{-}C_6H_3Me_3)]$ [5] although a number of clusters have been reported in which benzene co-ordinates as its fragmentation product viz. as a benzyne ligand, bonding to the metal atoms via two σ-bonds and one π-bond as in $[Os_3(\mu_2\text{-}AsMe_2)(\mu_2\text{-}H)(CO)_9(\mu_3\text{-}\eta^2\text{-}C_6H_4)]$ [6], $[Os_3(\mu_2\text{-}SMe)(\mu_2\text{-}H)(CO)_9(\mu_3\text{-}\eta^2\text{-}C_6H_4)]$ [7] and $[Os_3(\mu_2\text{-}H)_2(CO)_9(\mu_3\text{-}\eta^2\text{-}C_6H_4)]$ [8]. Significantly, it has been established more recently

0022-328X/91/$03.50

that arenes may also adopt bridging or capping co-ordination modes in bonding to metal clusters, bridging across the edge of a cluster or a dinuclear compound as found in $[Ru_2(\mu\text{-}PPh_2)(\mu\text{-}H)(\eta^5\text{-}C_5Me_5)_2(\mu\text{-}\eta^2:\eta^2\text{-}C_6H_6]$ [9], $[V_2(\eta^5\text{-}C_5H_5)_2H_2(\mu\text{-}\eta^4:\eta^4\text{-}C_6H_6)]$ [10] and $[Fe_2(\eta^5\text{-}C_5H_5)_2(\mu\text{-}\eta^4:\eta^4\text{-}C_6Me_6)]$ [11] or co-ordinating symmetrically as a triene to the face of a cluster as found in $[Ru_6(C)(CO)_{11}(\mu_3\text{-}\eta^2:\eta^2:\eta^2\text{-}C_6H_6)(\eta^6\text{-}C_6H_6)]$ [12], $[Os_3(CO)_9(\mu_3\text{-}\eta^2:\eta^2:\eta^2\text{-}C_6H_6)]$ [12], $[Os_3(CO)_8(L)(\mu_3\text{-}\eta^2:\eta^2:\eta^2\text{-}C_6H_6)]$ ($L = PR_3$, C_5H_5N, alkenes, etc) [13] and $[Co_3(\eta^5\text{-}C_5Me_5)_3(\mu_3\text{-}\eta^2:\eta^2:\eta^2\text{-}C_6H_5CH{=}CHMe)]$ [14].

A recognised method of preparation of phosphido-bridged or phosphinidene-capped metal carbonyl clusters likewise involves the direct reaction of metal carbonyls with secondary or primary phosphines. Thus treatment of $[Ru_3(CO)_{12}]$ with an equimolar amount of PPh_2H under mild conditions in the presence of a catalytic amount of sodium benzophenone ketyl has been observed to lead to the formation of the monosubstituted derivative $[Ru_3(CO)_{11}(PPh_2H)]$ which readily decarbonylates and rearranges to the bridged diphenylphosphido species $[Ru_3(\mu_2\text{-}PPh_2)(\mu_2\text{-}H)(CO)_{10}]$ in heptane at 60 °C [15]. Similarly, reaction of $[Ru_3(CO)_{12}]$ with phenylphosphine has been found to afford trinuclear phenylphosphinidene-capped products at temperatures of 80 °C and less [16–18]. An increase in the temperature of these reactions leads to the condensation of the metal atom frameworks (vide supra) and the formation of higher nuclearity products and indeed the tetra-, penta, hexa-, hepta- and octanuclear derivatives $[Ru_4(\mu_4\text{-}PPh)_2(\mu_2\text{-}CO)(CO)_{10}]$, $[Ru_5(\mu_4\text{-}PPh)(CO)_{15}]$, $[Ru_6(\mu_4\text{-}PPh)_2(\mu_3\text{-}PPh)_2(CO)_{12}]$, $[Ru_7(\mu_4\text{-}PPh)_2(CO)_{18}]$ and $[Ru_8(\mu_8\text{-}P)(\mu_2\text{-}\eta^1,\eta^6\text{-}CH_2Ph)(\mu_2\text{-}CO)(CO)_{17}]$ have been isolated from the reaction of $[Ru_3(CO)_{12}]$ with PPh_2H in toluene under reflux [19].

It is to be expected that the use of high boiling point arenes in these reactions might lead to the simultaneous formation of π-arene derivatives and this has in fact now been observed for the reaction of $[Ru_3(CO)_{12}]$ with $PPhH_2$ in toluene under reflux. The details of the synthesis and characterization of these compounds are reported here.

Results and discussion

We have shown previously that the reaction of $[Ru_3(CO)_{12}]$ with an equimolar amount of $PPhH_2$ in toluene under reflux for 12–24 hours is complex and affords a reaction mixture which gives a large number of bands on column chromatographic treatment [16]. Eight of these bands (in order of elution: yellow, green, brown (i), green-brown, brown (ii), purple, dark green and brown (iii)) were distinct and could be separated although the residues from three of them (green-brown, brown (ii) and brown (iii)) could not be isolated in crystalline form and as a consequence could not be characterized. The products isolated from the remaining five bands were characterized as $[Ru_3(\mu_3\text{-}PPh)(\mu_2\text{-}H)_2(CO)_9]$ (**1**) (yellow band), $[Ru_4(\mu_4\text{-}PPh)_2(\mu_2\text{-}CO)(CO)_{10}]$ (**2**) (purple band), $[Ru_5(\mu_4\text{-}PPh)(CO)_{15}]$ (**3**) (first green band), $[Ru_5(\mu_4\text{-}PPh)\{\mu_2\text{-}PPh(OPr^n)\}(\mu\text{-}H)(CO)_{13}]$ (**4**) (first brown band) and $[Ru_7(\mu_4\text{-}PPh)_2(CO)_{18}]$ (**5**) (second green band), respectively.

The yield of the pentanuclear species $[Ru_5(\mu_4\text{-}PPh)(CO)_{15}]$ (**3**) was observed to be considerably higher for the 24 hour reaction (12–15%) than for the 12 hour one and thus, with the aim of optimizing the yield of this compound, $[Ru_3(CO)_{12}]$ was reacted with $PPhH_2$ in toluene under reflux for 40 hours, molar ratios of 1 : 1 and

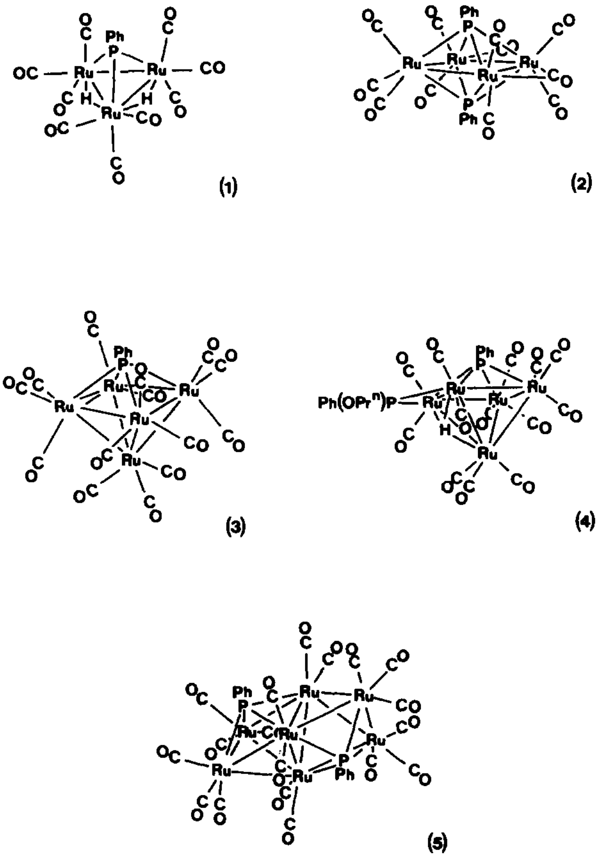

Scheme 1.

5 : 3 being employed. Extraction of the product mixture with warm petroleum ether and column chromatographic treatment of the extractant resulted in the separation of four distinct bands (in order of elution: green (i), purple, green (ii) and brown). The first band was established to contain $[Ru_5(\mu_4\text{-}PPh)(CO)_{15}]$ while the purple band was shown to contain $[Ru_4(\mu_4\text{-}PPh)_2(\mu_2\text{-}CO)(CO)_{10}]$ (**2**). The brown band afforded a dull brown powder which could not be purified and was not investigated further.

The second green band afforded a product for which the analytical data were consistent with the stoichiometry $[Ru_5(PPh)(CO)_{12}(C_6H_5Me)]$. The $^{31}P\{^1H\}$ NMR spectrum of this compound contains a singlet at 441.6 ppm, relative to H_3PO_4, and this is interpreted in terms of the phenylphosphinidene ligand capping four ruthenium atoms similar to that established [20] for $[Ru_5(\mu_4\text{-}PPh)(CO)_{15}]$ which exhibits a singlet at 434 ppm in its $^{31}P\{^1H\}$ NMR spectrum and of the compound being, in fact, a substituted derivative of the latter with a toluene ligand having replaced three of the carbonyl groups.

Confirmation of the identity of this compound was achieved by means of an X-ray crystal structure determination and the stereochemistry of the species, as established, is illustrated in Fig. 1. The five metal atoms adopt a square-pyramidal

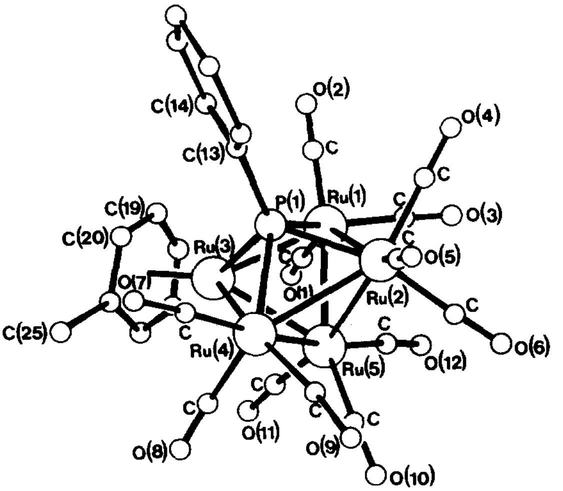

Fig. 1. The molecular stereochemistry of $[Ru_5(\mu_4\text{-}PPh)(CO)_{12}(\eta^6\text{-}C_6H_5Me)]$ showing the atom labelling scheme; the labelling of the carbonyl carbon atoms is the same as that for the corresponding oxygen atoms.

geometry with the square basal plane being capped by the phenylphosphinidene ligand. The ruthenium–ruthenium distances range from 2.774(1) to 2.901(1) Å, very similar to the range of distances observed for the parent species $[Ru_5(\mu_4\text{-}PPh)(CO)_{15}]$ [20]. The toluene ligand is co-ordinated to one of the basal ruthenium atoms {Ru(3)} in the η^6 co-ordination mode with the ruthenium–carbon distances ranging from 2.209(8) to 2.293(8) Å. Significantly, the distance between Ru(3) and the apical Ru(5) atom {2.901(1) Å} is longer than any of the other apical–basal Ru–Ru distances {2.774(1), 2.788(1) and 2.864(1) Å} while the distances between Ru(3) and the two adjacent basal ruthenium atoms {Ru(1) and Ru(4)} are shorter {2.815(1) and 2.838(1) Å} than the other two basal–basal Ru–Ru distances {2.869(1) and 2.875(1) Å}. The phosphorus of the phenylphosphinidene ligand is essentially symmetrically disposed with respect to the four basal ruthenium atoms although the distance between it and Ru(3) {2.276(2) Å} is significantly less than the other three Ru–P distances {2.362(2), 2.388(2) and 2.396(2) Å}.

In the selection of the crystals of $[Ru_5(\mu_4\text{-}PPh)(CO)_{12}(\eta^6\text{-}C_6H_5Me)]$ for the structure determination, crystals of a different form were identified in spite of their being present in negligible amounts. Use of these crystals for a structure determination led to the discovery that they corresponded to a second π-toluene complex and in particular to a π-toluene derivative of the heptanuclear cluster $[Ru_7(\mu_4\text{-}PPh)_2(CO)_{18}]$ viz. $[Ru_7(\mu_4\text{-}PPh)_2(CO)_{15}(\eta^6\text{-}C_6H_5Me)]$. The stereochemistry of this species is illustrated in Fig. 2 and is based on that of its parent, $[Ru_7(\mu_4\text{-}PPh)_2(CO)_{18}]$ [21], with the seven ruthenium atoms defining a condensed polyhedron consisting of two square pyramidal Ru_5 units sharing a triangular face defined by Ru(1), Ru(3) and Ru(6), and with each basal plane being capped by a phenylphosphinidene ligand. A number of structural features warrant comment. Firstly, as found for $[Ru_5(\mu_4\text{-}PPh)(CO)_{12}(\eta^6\text{-}C_6H_5Me)]$, the toluene ligand is co-ordinated to one of the basal ruthenium atoms {Ru(2)} in the η^6 co-ordination mode. Secondly, the distance between the ruthenium atom containing the co-

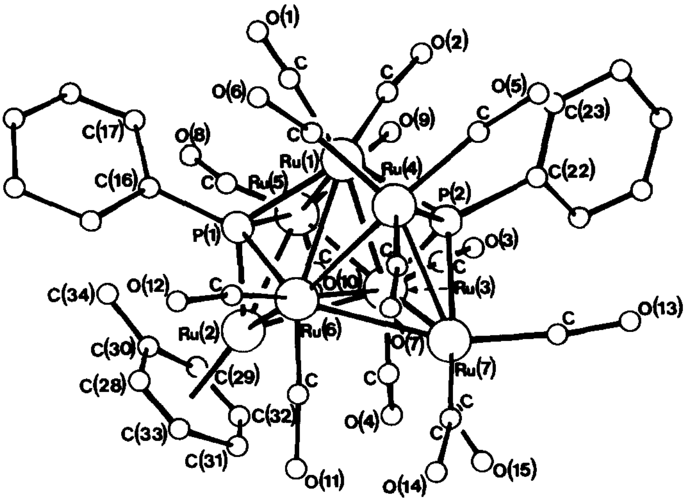

Fig. 2. The molecular stereochemistry of $[Ru_7(\mu_4\text{-PPh})_2(CO)_{15}(\eta^6\text{-}C_6H_5Me)]$ showing the atom labelling scheme; the labelling of the carbonyl carbon atoms is the same as that for the corresponding oxygen atoms.

ordinated toluene i.e. Ru(2) and the adjacent apical ruthenium atom {2.896(2) Å} is longer than the other apical–basal Ru–Ru distances for the same Ru_5 unit {2.756(3), 2.771(2) and 2.882(2) Å} or, for that matter, than those of the other Ru_5 unit {2.771(2), 2.783(2), 2.828(3) and 2.888(2) Å}. Thirdly, the distances between Ru(2) and the two adjacent basal ruthenium atoms {Ru(5) and Ru(6)} are shorter {2.818(3) and 2.829(3) Å} than the other two basal–basal Ru–Ru distances for the same Ru_5 fragment {2.872(2) and 2.888(2) Å} as well as being shorter than the basal–basal Ru–Ru distances for the other Ru_5 unit {2.846(2), 2.882(2), 2.907(2) and 2.938(3) Å}. Fourthly, the distance between the appropriate phosphorus {P(1)} and the ruthenium containing the co-ordinated toluene {2.298(6) Å} is again shorter than the other three Ru–P distances for the same Ru_5P moiety {2.349(6), 2.351(5) and 2.397(5) Å}.

The number and size of the crystals of $[Ru_7(\mu_4\text{-PPh})_2(CO)_{15}(\eta^6\text{-}C_6H_5Me)]$ were too small to permit their separation from the crystals of $[Ru_5(\mu_4\text{-PPh})(CO)_{12}(\eta^6\text{-}C_6H_5Me)]$ but the $^{31}P\{^1H\}$ NMR spectra of several of the batches of $[Ru_5(\mu_4\text{-PPh})(CO)_{12}(\eta^6\text{-}C_6H_5Me)]$ exhibited weak peaks at 458.9 and 460.5 ppm which could be assigned to $[Ru_7(\mu_4\text{-PPh})_2(CO)_{15}(\eta^6\text{-}C_6H_5Me)]$.

Experimental

All reactions and manipulations were carried out under an atmosphere of nitrogen using Schlenk tube techniques. Solvents were purified and dried using standard procedures. $[Ru_3(CO)_{12}]$ was synthesized from $RuCl_3 \cdot xH_2O$ by a procedure developed by Mr P. Loveday of the University of Cambridge while $PPhH_2$ was obtained commercially and used without further purification. Infrared spectra were recorded on Perkin–Elmer 457 and 283 grating spectrometers while $^{31}P\{^1H\}$ NMR spectra were measured on a Varian FT80A instrument. Light petroleum with a b.p. range 60–80 °C was used throughout.

Synthesis of $[Ru_4(\mu_4\text{-}PPh)_2(\mu_2\text{-}CO)(CO)_{10}]$, $[Ru_5(\mu_4\text{-}PPh)(CO)_{15}]$, $[Ru_5(\mu_4\text{-}PPh)(CO)_{12}(\eta^6\text{-}C_6H_5Me)]$ *and* $[Ru_7(\mu_4\text{-}PPh)_2(CO)_{15}(\eta^6\text{-}C_6H_5Me)]$

A solution of $[Ru_3(CO)_{12}]$ (0.50 g, 0.78 mmol) and $PPhH_2$ (0.086 g, 0.78 mmol or 0.051 g, 0.47 mmol) in toluene (ca. 100 cm^3) was refluxed for 40 h. The solvent was removed under reduced pressure and the dark brown residue extracted with six

Table 1

Fractional atomic coordinates ($\times 10^4$) and isotropic temperature factors (Å$^2 \times 10^3$) for $[Ru_5(\mu_4\text{-}PPh)(CO)_{12}(\eta^6\text{-}C_6H_5Me)]$

	x	*y*	*z*	*U*
Ru(1)	1833(1)	3016(1)	1223(1)	28(1) [a]
Ru(2)	4384(1)	3650(1)	648(1)	29(1) [a]
Ru(3)	3368(1)	1825(1)	1923(1)	26(1) [a]
Ru(4)	5863(1)	2341(1)	1233(1)	30(1) [a]
Ru(5)	3521(1)	2118(1)	303(1)	27(1) [a]
P(1)	4085(2)	3065(1)	1845(1)	26(1) [a]
O(1)	−145(6)	1671(3)	986(3)	55(1)
O(2)	208(7)	3841(4)	2437(4)	66(2)
O(3)	465(7)	4005(4)	−7(4)	66(2)
O(4)	2963(8)	5147(4)	1005(4)	76(2)
O(5)	7192(8)	4433(4)	763(4)	80(2)
O(6)	4101(7)	3762(4)	−1065(4)	68(2)
O(7)	8053(8)	2442(4)	2490(4)	73(2)
O(8)	6247(7)	635(4)	982(4)	68(2)
O(9)	7935(7)	2734(3)	0(4)	61(2)
O(10)	5585(8)	1806(4)	−948(5)	78(2)
O(11)	2882(7)	428(4)	359(4)	60(2)
O(12)	1287(7)	2461(4)	−885(4)	63(2)
C(1)	618(8)	2164(4)	1089(4)	38(2)
C(2)	814(8)	3517(4)	1971(5)	43(2)
C(3)	986(9)	3645(5)	476(5)	48(2)
C(4)	3492(9)	4574(5)	872(5)	49(2)
C(5)	6105(9)	4123(5)	711(5)	49(2)
C(6)	4167(8)	3682(4)	−422(4)	38(2)
C(7)	7238(8)	2434(4)	2021(5)	43(2)
C(8)	6030(9)	1289(4)	1105(5)	44(2)
C(9)	7105(9)	2629(4)	462(5)	44(2)
C(10)	4816(9)	1933(4)	−438(5)	44(2)
C(11)	3087(8)	1089(4)	374(4)	39(2)
C(12)	2111(8)	2345(4)	−415(4)	35(2)
C(13)	4509(7)	3604(4)	2709(4)	34(2)
C(14)	3620(8)	3601(4)	3332(4)	40(2)
C(15)	3974(9)	4021(5)	3977(5)	47(2)
C(16)	5225(10)	4427(5)	4023(5)	60(2)
C(17)	6145(10)	4408(5)	3393(5)	58(2)
C(18)	5756(10)	4011(5)	2747(5)	55(2)
C(19)	2321(8)	1732(4)	3029(5)	45(2)
C(20)	3765(8)	1564(4)	3142(5)	42(2)
C(21)	4419(8)	960(4)	2730(5)	44(2)
C(22)	3582(8)	575(4)	2169(5)	43(2)
C(23)	2161(8)	738(4)	2069(4)	41(2)
C(24)	1547(9)	1299(4)	2512(5)	43(2)
C(25)	5892(11)	728(6)	2913(6)	65(3)

[a] $U_{eq} = \frac{1}{3}\Sigma_i\Sigma_j U_{ij} a_i^* a_j^* (\mathbf{a}_i \cdot \mathbf{a}_j)$.

aliquots (ca. 50 cm^3 each) of warm light petroleum (ca. 60 ° C). The extracts were combined and the combined solution was concentrated and transferred to a silica gel column (Merck Kieselgel 60). The column was eluted initially with light petroleum and subsequently with light petroleum–dichloromethane mixtures of increasing dichloromethane content to afford four bands which were collected.

Band (1) (green) afforded $[Ru_5(\mu_4\text{-}PPh)(CO)_{15}]$ [16,20] as green crystals. Yield: 1 : 1 molar ratio, 100–120 mg; 5 : 3 molar ratio, 60–70 mg.

Band (2) (purple) afforded purple crystals of $[Ru_4(\mu_4\text{-}PPh)_2(\mu_2\text{-}CO)(CO)_{10}]$ [16]. Yield: 1 : 1 and 5 : 3 molar ratio, 40–50 mg.

Band (4) (brown) gave a brown powder which was not investigated further.

The solution from the second band was concentrated and cooled to 0 ° C to give green crystals of $[Ru_5(\mu_4\text{-}PPh)(CO)_{12}(\eta^6\text{-}C_6H_5Me)]$. Recrystallization was effected from dichloromethane–light petroleum. Yield: 1 : 1 molar ratio, 10–20 mg; 5 : 3 molar ratio, 80–100 mg. Anal. Calcd. for $C_{25}H_{13}O_{12}PRu_5.CH_2Cl_2$: C, 27.7; H, 1.33. Found: C, 27.7; H, 1.38%. ν(CO): 2071m, 2035vs, 2012s, 1994w,br, 1975sh, 1967w,br cm^{-1} (in C_6H_{12}). $^{31}P\{^1H\}$ NMR: 441.6s (δ scale, relative to H_3PO_4, in $CDCl_3$).

Crystals of $[Ru_7(\mu_4\text{-}PPh)_2(CO)_{15}(\eta^6\text{-}C_6H_5Me)] \cdot CH_2Cl_2$ which were used in the crystallographic study were isolated from one of the batches of crystals of $[Ru_5(\mu_4\text{-}PPh)(CO)_{12}(\eta^6\text{-}C_6H_5Me)]$.

X-Ray crystal structure determination of $[Ru_5(\mu_4\text{-}PPh)(CO)_{12}(\eta^6\text{-}C_6H_5Me)]$

A crystal grown from CH_2Cl_2–light petroleum and of dimensions 0.17 × 0.23 × 0.60 mm was used for the data collection. Crystal data: $C_{25}H_{13}O_{12}PRu_5$, *M* 1041.67, monoclinic, *a* 9.545(1), *b* 17.478(3), *c* 17.587(3) Å, β 91.00(1)°, *U* 2933.5(7) $Å^3$, D_c 2.358 g cm^{-3}, $Z = 4$, space group $P2_1/n$ (non-standard setting No. 14), Mo-K_α radiation (λ 0.71069Å), μ(Mo-K_α) 25.66 cm^{-1}, $F(000) = 1976$.

Table 2

Selected interatomic distances (Å) and angles (°) for $[Ru_5(\mu_4\text{-}PPh)(CO)_{12}(\eta^6\text{-}C_6H_5Me)]$

Ru(1)–Ru(2)	2.875(1)	Ru(1)–Ru(3)	2.815(1)
Ru(1)–Ru(5)	2.788(1)	Ru(2)–Ru(4)	2.869(1)
Ru(2)–Ru(5)	2.864(1)	Ru(3)–Ru(4)	2.838(1)
Ru(3)–Ru(5)	2.901(1)	Ru(4)–Ru(5)	2.774(1)
Ru(1)–P(1)	2.396(2)	Ru(2)–P(1)	2.362(2)
Ru(3)–P(1)	2.276(2)	Ru(4)–P(1)	2.388(2)
Ru(3)–C(19)	2.209(8)	Ru(3)–C(20)	2.218(8)
Ru(3)–C(21)	2.293(8)	Ru(3)–C(22)	2.236(8)
Ru(3)–C(23)	2.240(7)	Ru(3)–C(24)	2.236(8)
P(1)–C(13)	1.828(7)	C(19)–C(20)	1.42(1)
C(20)–C(21)	1.43(1)	C(21)–C(22)	1.43(1)
C(22)–C(23)	1.39(1)	C(23)–C(24)	1.39(1)
C(19)–C(24)	1.39(1)	C(21)–C(25)	1.49(1)

Ru–C(O) distances fall in the range 1.840(9)–1.900(7)
C–O distances fall in the range 1.14(1)–1.19(1)
C(Ph)–C(Ph) distances fall in the range 1.38(1)–1.43(1)

Ru(2)–Ru(1)–Ru(3)	90.1(0)	Ru(1)–Ru(2)–Ru(4)	88.9(0)
Ru(1)–Ru(3)–Ru(4)	90.7(0)	Ru(2)–Ru(4)–Ru(3)	89.7(0)

Table 3

Fractional atomic coordinates ($\times 10^4$) and equivalent isotropic temperature factors ($Å^2 \times 10^3$) fo $[Ru_7(\mu_4\text{-PPh})_2(CO)_{15}(\eta^6\text{-}C_6H_5Me)]\cdot CH_2Cl_2$

	x	y	z	U_{eq}
Ru(1)	2259(1)	734(1)	3322(1)	38(1)
Ru(2)	588(1)	1792(1)	1542(1)	51(1)
Ru(3)	2717(1)	1765(1)	2280(1)	43(1)
Ru(4)	3330(1)	−47(1)	2201(1)	43(1)
Ru(5)	1169(1)	1867(1)	3346(1)	52(1)
Ru(6)	1832(1)	746(1)	1451(1)	42(1)
Ru(7)	3917(2)	974(1)	1238(1)	51(1)
P(1)	707(4)	982(2)	2487(4)	39(1)
P(2)	3774(4)	940(3)	2736(3)	37(1)
O(1)	1309(17)	−291(10)	4152(14)	90(6) [a]
O(2)	3205(16)	987(10)	5136(15)	91(6) [a]
O(3)	3823(16)	2659(10)	3528(13)	87(6) [a]
O(4)	2631(21)	2826(13)	1100(18)	129(9) [a]
O(5)	5155(17)	−688(10)	3104(15)	96(6) [a]
O(6)	1905(19)	−1097(12)	2571(17)	121(8) [a]
O(7)	3602(19)	−766(12)	589(17)	114(8) [a]
O(8)	−814(21)	1878(12)	4155(18)	117(8) [a]
O(9)	2405(20)	2257(12)	5008(17)	120(8) [a]
O(10)	1134(20)	3219(12)	2820(18)	120(8) [a]
O(11)	1900(24)	1172(15)	−355(22)	157(11) [a]
O(12)	887(18)	−429(11)	663(16)	102(7) [a]
O(13)	6254(25)	889(14)	1597(21)	153(11) [a]
O(14)	3964(19)	368(11)	−491(17)	112(8) [a]
O(15)	4214(39)	2077(23)	322(33)	243(22) [a]
C(1)	1654(20)	60(12)	3857(18)	62(7) [a]
C(2)	2762(18)	887(11)	4440(16)	54(6) [a]
C(3)	3362(19)	2305(12)	3063(16)	59(6) [a]
C(4)	2667(26)	2362(16)	1448(22)	92(10) [a]
C(5)	4413(24)	−438(14)	2830(21)	83(8) [a]
C(6)	2428(24)	−683(14)	2530(20)	80(8) [a]
C(7)	3543(23)	−477(14)	1207(21)	81(8) [a]
C(8)	−98(25)	1878(15)	3755(22)	84(9) [a]
C(9)	1963(20)	2076(12)	4406(18)	59(7) [a]
C(10)	1147(22)	2686(14)	3054(19)	75(8) [a]
C(11)	1917(24)	957(14)	418(22)	83(9) [a]
C(12)	1311(26)	5(16)	1027(23)	95(10) [a]
C(13)	5324(21)	924(12)	1391(18)	65(7) [a]
C(14)	4031(26)	609(16)	172(24)	92(10) [a]
C(15)	3790(57)	1761(33)	724(48)	220(30) [a]
C(16)	−444(14)	534(8)	2638(12)	31(4) [a]
C(17)	−788(18)	454(11)	3505(15)	52(6) [a]
C(18)	−1604(23)	138(14)	3571(20)	79(8) [a]
C(19)	−2116(26)	−124(16)	2959(23)	91(10) [a]
C(20)	−1887(23)	−91(14)	2072(20)	81(9) [a]
C(21)	−984(19)	270(11)	1971(16)	59(6) [a]
C(22)	4990(16)	1064(10)	3486(14)	45(5) [a]
C(23)	5245(19)	636(11)	4175(17)	61(6) [a]
C(24)	6144(20)	716(12)	4744(17)	63(7) [a]
C(25)	6743(17)	1217(11)	4527(15)	52(6) [a]
C(26)	6474(20)	1638(12)	3841(18)	69(7) [a]
C(27)	5578(16)	1538(9)	3316(14)	41(5) [a]

Table 3 (continued)

	x	y	z	U_{eq}
C(28)	−820(20)	1597(12)	677(17)	65(7) [a]
C(29)	−541(22)	2567(14)	1360(19)	77(8) [a]
C(30)	−1035(19)	1982(12)	1337(17)	61(7) [a]
C(31)	473(18)	2281(12)	225(16)	56(6) [a]
C(32)	238(19)	2675(11)	769(16)	60(6) [a]
C(33)	−158(24)	1727(15)	167(21)	84(9) [a]
C(34)	−1819(32)	1903(19)	1979(28)	121(13) [a]
Cl(1)	2030(27)	1748(11)	7656(19)	352(15)
Cl(2)	336(24)	1563(16)	6549(35)	534(25)
C(35)	958(34)	1710(21)	7697(29)	110(13) [a]

[a] Isotropic temperature factor.

$U_{eq} = \frac{1}{3}\Sigma_i \Sigma_j U_{ij} a_i^* a_j^* (\mathbf{a}_i \cdot \mathbf{a}_j)$.

Intensity data were collected on a Nonius CAD-4 diffractometer using graphite monochromated Mo-K_α radiation. A least-squares fit of 25 high-angle reflections ($\theta > 12°$) was used to obtain accurate cell constants. Diffraction intensities were measured in the range $3 \leq 2\theta \leq 23°$ using the ω–2θ scan technique, with background counts made for half the total scan time on each side of the peak. Three standard reflections, measured every hour, showed no decrease in intensity during data collection. Lorentz and polarisation as well as absorption corrections, the latter obtained by analysis of nine azimuthal scans, were applied. Of the 3945 unique reflections measured, 3743 were classed as observed [$I > 3\sigma(I)$] and these were used for the solution and refinement of the structure.

The structure was solved by conventional Patterson and Fourier techniques. Hydrogen atoms were not located. The Ru and P atoms were assigned anisotropic thermal parameters while the remaining non-hydrogen atoms were assigned isotropic thermal parameters. A weighted full-matrix least-squares refinement (203 variables) converged at $R = 0.041$, $R_w = 0.057$, with the weights $w = 1/[\sigma^2(F) + 0.003^2]$ ($\sigma(F)$ from counting statistics). A final difference Fourier was featureless with a maximum peak height of 1.0 eÅ^{-3}. Complex neutral scattering factors were taken from ref. 22, and the program SHELX-76 [23] was used for the calculations. Atomic co-ordinates are given in Table 1 and selected bond distances and angles in Table 2.

X-Ray crystal structure determination of $[Ru_7(\mu_4\text{-}PPh)_2(CO)_{15}(\eta^6\text{-}C_6H_5Me)] \cdot CH_2Cl_2$

A crystal grown from CH_2Cl_2–light petroleum and of dimensions 0.15 × 0.19 × 0.48 mm was used for the data collection. Crystal data: $C_{35}H_{20}Cl_2O_{15}P_2Ru_7$, M 1520.84, monoclinic, a 13.091(2), b 21.988(2), c 15.468(2) Å, β 96.20(1)°, U 4426.1(8) Å^3, D_c 2.282 g cm^{-3}, $Z = 4$, space group $P2_1/n$ (non-standard setting No. 14), Mo-K_α radiation (λ 0.71069Å), μ(Mo-K_α) 25.22 cm^{-1}, $F(000) = 2888$.

Intensity data were collected as above. Of the 6014 unique reflections measured 5768 were classed as observed [$I > 3\sigma(I)$] and these were used in the solution and refinement of the structure.

The structure was solved by conventional Patterson and Fourier techniques. Hydrogen atoms were not located. The Ru and P atoms were assigned anisotropic

Table 4

Selected interatomic distances (Å) and angles (°) for $[Ru_7(\mu_4\text{-}PPh)_2(CO)_{15}(\eta^6\text{-}C_6H_5Me)]\cdot CH_2Cl_2$

Ru(1)-Ru(3)	2.882(2)	Ru(1)-Ru(4)	2.907(2)
Ru(1)-Ru(5)	2.872(2)	Ru(1)-Ru(6)	2.888(2)
Ru(2)-Ru(3)	2.896(2)	Ru(2)-Ru(5)	2.818(3)
Ru(2)-Ru(6)	2.829(3)	Ru(3)-Ru(5)	2.756(3)
Ru(3)-Ru(6)	2.771(3)	Ru(3)-Ru(7)	2.938(3)
Ru(4)-Ru(6)	2.783(2)	Ru(4)-Ru(7)	2.846(2)
Ru(6)-Ru(7)	2.828(3)	Ru(1)-P(1)	2.351(5)
Ru(2)-P(1)	2.298(6)	Ru(5)-P(1)	2.397(5)
Ru(6)-P(1)	2.349(6)	Ru(1)-P(2)	2.313(6)
Ru(3)-P(2)	2.342(6)	Ru(4)-P(2)	2.374(6)
Ru(7)-P(2)	2.345(6)	Ru(2)-C(28)	2.20(3)
Ru(2)-C(29)	2.25(3)	Ru(2)-C(30)	2.15(3)
Ru(2)-C(31)	2.29(3)	Ru(2)-C(32)	2.30(3)
Ru(2)-C(33)	2.25(3)	P(1)-C(16)	1.84(2)
P(2)-C(22)	1.89(2)	C(28)-C(30)	1.38(3)
C(28)-C(33)	1.27(4)	C(29)-C(30)	1.44(4)
C(29)-C(32)	1.46(4)	C(30)-C(34)	1.51(5)
C(31)-C(32)	1.27(3)	C(31)-C(33)	1.47(4)

Ru-C(O) distances fall in the range 1.68(3)-1.93(3)
C-O distances fall in the range 1.02(3)-1.28(4)
C(Ph)-C(Ph) distances fall in the range 1.32(3)-1.47(3)

Ru(5)-Ru(1)-Ru(6)	87.8(1)	Ru(5)-Ru(2)-Ru(6)	90.1(1)
Ru(1)-Ru(4)-Ru(7)	91.2(1)	Ru(1)-Ru(5)-Ru(2)	91.0(1)
Ru(1)-Ru(6)-Ru(2)	90.4(1)	Ru(3)-Ru(7)-Ru(4)	89.4(1)

thermal factors while the remaining non-hydrogen atoms were assigned isotropic thermal factors. A weighted full-matrix least-squares refinement (300 variables) converged at $R = 0.104$, $R_w = 0.122$, with the weights $w = 43.8/[\sigma^2(F) + 0.00005F^2]$ ($\sigma(F)$ from counting statistics). A final difference Fourier was featureless with a maximum peak height of 2.3 $e\text{Å}^{-3}$. Complex neutral scattering factors were taken from ref. 22, and the program SHELX-76 [23] was used for the calculations. Atomic co-ordinates are given in Table 3 and selected bond distances and angles in Table 4.

Acknowledgements

The authors express their sincere thanks to the Foundation for Research Development of the South African Council for Scientific and Industrial Research and the University of Natal for financial support.

References

1 E.O. Fischer, K. Öfele, H. Essler, W. Frohlich, J.P.Mortensen and W. Semmlinger, Chem. Ber., 91 (1958) 2763.
2 B. Nicholls and M.C. Whiting, J. Chem. Soc., (1959) 551.
3 C.E. Anson, P.J. Bailey, G. Conole, B.F.G. Johnson, J. Lewis, M. McPartlin and H.R. Powell, J. Chem. Soc., Chem. Commun., (1989) 442.
4 B.F.G. Johnson, R.D. Johnston and J. Lewis, Chem. Commun., (1967) 1057; B.F.G. Johnson, R.D. Johnston and J. Lewis, J. Chem. Soc. (A), (1968) 2865.

5 R. Mason and W.R. Robinson, J. Chem. Soc., Chem. Commun., (1968) 468.
6 A.J. Deeming, I.P. Rothwell, M.B. Hursthouse and J.D.J. Backer-Dirks, J. Chem. Soc., Dalton Trans., (1981) 1879.
7 R.D. Adams, D.A. Katahira and L.-W. Yang, Organometallics, 1 (1982) 235.
8 R.J. Goudsmit, B.F.G. Johnson, J. Lewis, P.R. Raithby and M.J. Rosales, J. Chem. Soc., Dalton Trans., (1983) 2257.
9 H. Omori, H. Suzuki, Y. Take and Y. Moro-oka, Organometallics, 8 (1989) 1170.
10 K. Jonas, V. Wiskamp, Y.-H. Tsay and C. Krüger, J. Am. Chem. Soc., 105 (1983) 5480.
11 K. Jonas, G. Koepe, L. Schieferstein, R. Mynott, C. Krüger and Y.-H. Tsay, Angew. Chem., Int. Ed. Engl., 22 (1983) 620.
12 M.P. Gomez-Sal, B.F.G. Johnson, J. Lewis, P.R. Raithby and A.H. Wright, J. Chem. Soc., Chem. Commun., (1985) 1682.
13 M.A. Gallop, B.F.G. Johnson, J. Lewis and P.R. Raithby, J. Chem. Soc., Chem. Commun., (1987) 1809.
14 H. Wadepohl, K. Büchner and H. Pritzkow, Angew. Chem., Int. Ed. Engl., 26 (1987) 1259.
15 S.A. MacLoughlin, N.J. Taylor and A.J. Carty, Organometallics, 3 (1984) 392.
16 J.S. Field, R.J. Haines and D.N. Smit, J. Organomet. Chem., 224 (1982) C49; J.S. Field, R.J. Haines and D.N. Smit, J. Chem. Soc., Dalton Trans., (1988) 1315.
17 F. Iwasaki, M.J. Mays, P.R. Raithby, P.L. Taylor and P.J. Wheatley, J. Organomet. Chem., 213 (1981) 185.
18 K. Natarajan, O. Scheidsteger and G. Huttner, J. Organomet. Chem., 221 (1981) 301.
19 L.M. Bullock, J.S. Field, R.J. Haines, E. Minshall, M.H. Moore, F. Mulla, D.N. Smit and L.M. Steer, J. Organomet. Chem., 381 (1990) 429.
20 K. Natarajan, L. Zsolnai and G. Huttner, J. Organomet. Chem., 209 (1981) 85.
21 F. van Gastel, N.J. Taylor and A.J. Carty, J. Chem. Soc., Chem. Commun., (1987) 1049.
22 International Tables for X-Ray Crystallography, Vol. 4, Kynoch Press, Birmingham, England, 1974.
23 G.M. Sheldrick, SHELX-76, Program for Crystal Structure Determination, University of Cambridge, 1976.